Bioorganic & Medicinal Chemistry 19 (2011) 5446–5453

Contents lists available at ScienceDirect

Bioorganic & Medicinal Chemistry

journal homepage: www.elsevier.com/locate/bmc

Synthesis and characterization of tritylthioethanamine derivatives with potent KSP inhibitory activity

Delany Rodriguez [a], Chinnasamy Ramesh [b], Lauren H. Henson [a], Lori Wilmeth [a], Bj K. Bryant [b], Samuel Kadavakollu [b], Rebecca Hirsch [a], Johnelle Montoya [a], Porsha R. Howell [a], Jon M. George [b], David Alexander [b], Dennis L. Johnson [b], Jeffrey B. Arterburn [b], Charles B. Shuster [a,*]

[a] Department of Biology, New Mexico State University, Las Cruces, NM 88003, USA
[b] Department of Chemistry and Biochemistry, New Mexico State University, Las Cruces, NM 88003, USA

ARTICLE INFO

Article history:
Received 4 June 2011
Revised 21 July 2011
Accepted 25 July 2011
Available online 30 July 2011

Keywords:
Kinesin Spindle Protein (KSP)
Mitosis
Kinesin
Anti-mitotic
Cell division

ABSTRACT

Assembly of a bipolar mitotic spindle requires the action of class 5 kinesins, and inhibition or depletion of this motor results in mitotic arrest and apoptosis. *S*-Trityl-L-cysteine is an allosteric inhibitor of vertebrate Kinesin Spindle Protein (KSP) that has generated considerable interest due to its anti-cancer properties, however, poor pharmacological properties have limited the use of this compound. We have modified the triphenylmethyl and cysteine groups, guided by biochemical and cell-based assays, to yield new cysteinol and cysteamine derivatives with increased inhibitory activity, greater efficacy in model systems, and significantly enhanced potency against the NCI60 tumor panel. These results reveal a promising new class of conformationally-flexible small molecules as allosteric KSP inhibitors for use as research tools, with activities that provide impetus for further development as anti-tumor agents.

1. Introduction

Natural and synthetic small molecules that target the microtubule cytoskeleton have proven invaluable for investigating the mechanisms of cell division. Modulators of microtubule polymerization (such as colcimid and paciltaxel) interfere with cell division by altering microtubule dynamics, resulting in extended mitotic arrest and cell death.[5,6] Microtubule disrupters have proven to be effective chemotherapeutics, but because microtubules are essential for many cellular functions, their toxicity imposes limitations to their use as anti-cancer agents. More recently, attention has turned toward kinesins as potential targets for anti-proliferative drugs.[7–11] There are roughly 14 classes of kinesin motors,[12] whose functions range from vesicular transport to cell division, and RNA interference analysis of 25 *Drosophila* kinesins revealed that four members were involved in mitotic spindle assembly.[13] Most prominent of these is the class five kinesin, Kinesin Spindle Protein (KSP; also known as Kif11 or Eg5), a plus end-directed motor that separates the spindle poles early in mitosis.[14] KSP is antagonized by a minus end-directed kinesin known as KifC1,[15] and inhibition of KSP results in spindle collapse and formation of a monopolar spindle. Because chromosomes are unable to establish bioriented attachments to the spindle, the cell arrests in mitosis, and eventually dies by apoptosis.[16] Although there are reports that KSP plays a role in neuronal development,[17] there are no other known functions outside of mitosis in adults, making KSP an attractive target for chemotherapeutic intervention.

Anti-cancer drug screening and chemical biological approaches have identified a number of KSP inhibitors, including monastrol,[18] *S*-trityl-L-cysteine (STLC, **1**),[19,20] 3QC,[21] MK-0731,[22] ispinesib,[23] and K858[24] (Fig. 1) that exhibit no activity against the other kinesin family members. The allosteric site located between α helix 3 and loop 5 of the KSP motor domain in vertebrate organisms has been identified as the common site of action for monastrol, **1** and ispinesib.[1,4,25–29] The specificity of these compounds for KSP is associated with the extended loop 5 found only in class 5 kinesins.[29] Kinetic analyses indicate that these allosteric inhibitors act through a mechanism whereby ADP release and motor rebinding to the microtubule are blocked.[16,23,30] Loop 5 undergoes dynamic conformational shifts during the ATP binding and hydrolysis cycle, and it is thought that interactions with small molecules such as monastrol "lock" this loop into an ADP bound-like conformation.[1,4,31,32] While monastrol has not demonstrated efficacy at pharmacologically relevant concentrations, several compounds that exhibit anti-cancer activity have advanced to clinical trials.[22,33–38] However, recent characterization of drug-resistant variants of KSP raises concern that tumor cells may develop resistance over time.[1,3,4]

* Corresponding author.
E-mail address: cshuster@nmsu.edu (C.B. Shuster).

0968-0896/$ - see front matter © 2011 Elsevier Ltd. All rights reserved.
doi:10.1016/j.bmc.2011.07.054

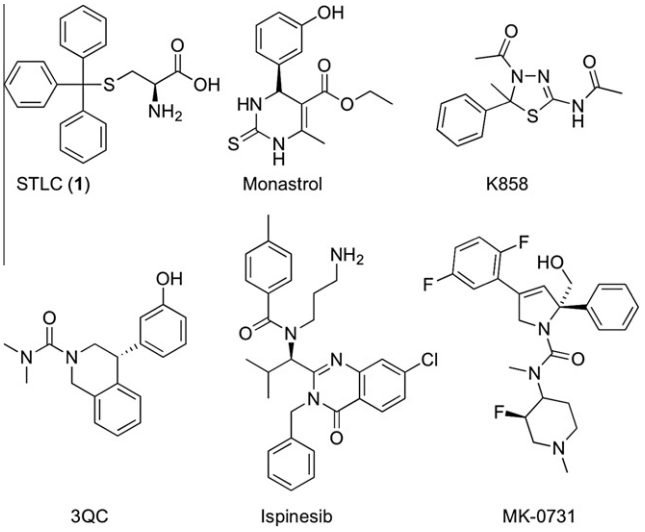

Figure 1. Representative structures of known KSP inhibitors, including STLC, monastrol, K858, 3QC, ispinesib, and MK-0731.

The cysteine derivative **1** represents a relatively simple scaffold with potent and reversible KSP inhibitory activity. Recent structure–activity analyses of STLC derivatives have been described and revealed the critical role of the trityl group for inhibitory activity.[39,40] The amphiphilic character of **1** results in poor water solubility and reduced permeability that affect bioavailability. We were interested in identifying related structures with increased inhibitory activity and improved physicochemical properties that would confer better water solubility and other drug-like characteristics. Herein, we describe the development of a new class of small, conformationally flexible KSP inhibitors based on the 2-(tritylthio)ethanamine scaffold. These compounds were effective inhibitors of human KSP in both biochemical and cell-based assays, as well as in nonmammalian model organisms. Two of the lead thioethanamine compounds **5** and **7** exhibited elevated anti-proliferative activity against the NCI60 panel of tumor cell lines and demonstrate the potential of this scaffold for the development of new anticancer therapeutics.

2. Chemistry

A series of STLC analogs have recently been evaluated in attempts to characterize structure–activity effects on KSP inhibition.[39–41] While structural alterations of the trityl group generally result in reduced inhibitory activity, the substitution of methyl, chloro, and methoxy groups in the *para*-position of the triphenylmethyl appendage was shown to increase the potency of STLC analogs. Carboxylic amides were found to function with similar inhibitory concentration values to the acids, but have not exhibited increased potency in the cellular assays.[42] Additionally, the individual *R*- and *S*-enantiomers of trityl-cysteine derived from L- and D-cysteine have previously been shown to inhibit KSP with equivalent potency.[16] Therefore, we focused our investigation on a series of novel thioethanamine compounds **4**–**7** related to **1**, but lacking the carboxylic group, seeking to achieve increased KSP inhibitory properties, more favorable physicochemical characteristics and increased cell permeability by eliminating the zwitterionic structure of the parent compound. The individual enantiomers of 4′-methoxytrityl derivatives **2** and **3** were prepared to allow comparison of their activities (Fig. 2) with **4**–**7**.

The thioethanamine derivatives were synthesized by the procedures shown in Scheme 1. Compounds **4–6** were prepared by

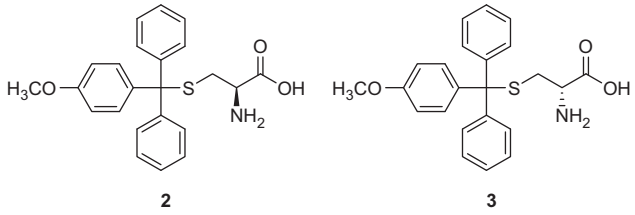

Figure 2. Enantiomers of *S*-4-methoxytritylcysteine evaluated as KSP inhibitors.

in situ reduction of cysteine to cysteinol with BH_3-THF, followed by quenching the excess borane reagent with DMF and selective *S*-alkylation with the appropriate trityl chloride. This efficient, two-step procedure avoids the formation of disulfide byproducts, and provided convenient access to the enantiomeric compounds **5** and **6** derived from L- and D-cysteine respectively. The achiral ethanamine derivative **7** was prepared using the published procedure for *S*-alkylation of cysteamine with 4-methoxytrityl chloride in trifluoroacetic acid.[43]

3. Results

Compounds **1–7** were tested for their ability to block human KSP activity in a biochemical ATPase assay[44] and a phenotypic assay in cultured HeLa cells (Table 1). The two assays provided a complementary assessment of direct inhibition of the motor, as well as indirectly reflecting membrane permeability and demonstrating efficacy in whole cells. The parent molecule **1** blocked the ATPase activity of recombinant human KSP with an IC_{50} of 0.62 μM, and in mitotic cells generated the stereotypical arrangement of microtubules radiating from the collapsed spindle poles with chromosomes arranged in a rosette pattern (Fig. 3, panel G). The 4′-methoxytrityl-derivative **2** exhibited increased potency as expected from recent reports.[39,40] The enantiomeric compound **3** derived from D-cysteine gave similar results in both assays, confirming the lack of stereochemical effects on inhibitory activity previously demonstrated for **1**.[16]

Evaluation of the inhibitory activity of the reduced cysteinol derivative **4** revealed an increase in potency associated with transformation of the carboxylic acid functional group to a primary alcohol that was comparable to incorporation of the 4'-methoxy-trityl group in **2**. An additive effect was observed for 4-methoxy-substituted cysteinol compound **5** that incorporates both of these modifications to achieve increased KSP inhibitory activity in both the biochemical and cellular assays. The enantiomer **6** derived from D-cysteine displayed equivalent activity in both biochemical and cell-based assays. The simple ethanamine compound **7** derived from cysteamine displayed the highest potency with an EC_{50} = 115 nM.

The parent compound **1** affects bipolar spindle formation without altering interphase microtubule dynamics or organization (Fig. 3B).[16] As illustrated in Figure 3, interphase microtubule morphology was normal for compounds **4**, **5** and **7** tested in the presence of 1 μM compound (Fig. 3C–E), whereas spindle morphology mirrored that of the parent compound (Fig. 3H–J). Additionally, it has been established that **1** displays no activity against other kinesin family members.[16,19] Compounds **4** and **5** were similarly tested for inhibitory activity against a selected panel of mitotic kinesins (mammalian centromere-associated kinesin (MCAK), centromeric protein E (CENP-E) and chromokinesin), with no measurable inhibition detected (not shown), suggesting that selectivity for class 5 kinesins was retained by the cysteinol derivatives.

KSP is a bipolar, homotetrameric motor whose nucleotide hydrolysis cycle is disrupted when treated with allosteric inhibi-

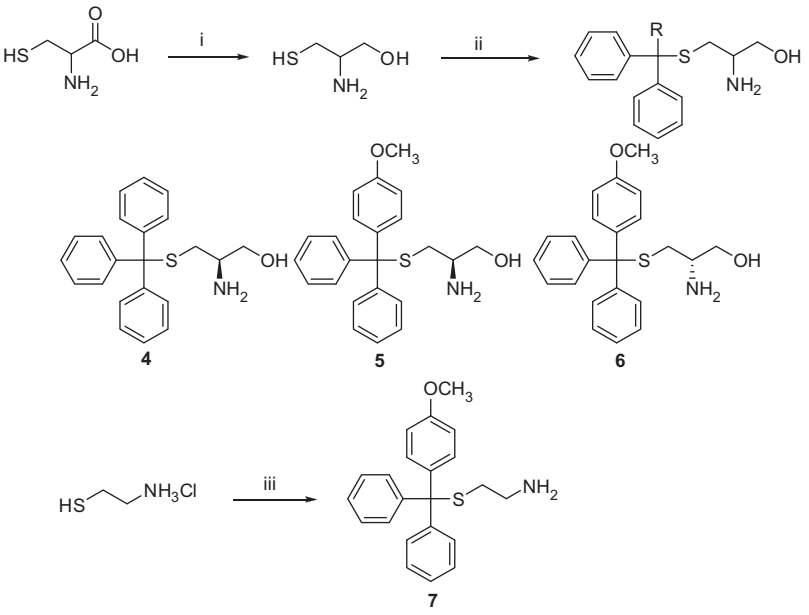

Scheme 1. Reagents and conditions: (i) BH_3-THF 0 °C – RT, DMF quench (ii) **4**, 88% yield from L-cysteine and trityl chloride; **5**, 91% yield from L-cysteine and 4-methoxytrityl chloride; **6**, 92% yield from D-cysteine and 4-methoxytrityl chloride; (iii) **7**, 96% yield from 4-methoxytrityl chloride, CF_3CO_2H.[43]

Table 1
IC_{50} values for inhibition of microtubule-stimulated KSP ATPase activity and EC_{50} values for mitotic arrest in cell-based assays for compounds **1**–**7**

Compound	ATPase activity [μM]	Cell-based assay [μM]
1	0.62	1.72
2	0.27	0.23
3	0.23	0.60
4	0.31	0.294
5	0.127	0.190
6	0.130	0.160
7	0.136	0.115

tors such as **1**, monastrol and ispinesib.[16,23,30] Kinetic analysis of motor inhibition predicts that KSP remains locked in the ADP bound state,[16,23,45] blocking motor rebinding and leading to a predicted loss of motor from spindle microtubules. To determine whether the cysteinol derivatives had a similar effect on KSP dynamics, cells were treated with **1** or **5** and probed for KSP localization with anti-KSP antibodies, using EB1 antibodies to label microtubules (Fig. 4). Similar to reports of monastrol-treated cells,[46] KSP was observed clustering at the center of the monopole upon treatment with either compound (Fig. 4A, D, G, J, M, and P). Both compounds displayed a dose-dependent depletion of KSP from the spindle, with **5** exhibiting a 1.63-fold increase in clearance of KSP over **1** (Fig. 4F J, M, and P), consistent with the biochemical- and cell-based assays (Table 1). Thus, the behavior of KSP in the presence of this cysteinol derivative was consistent with a mechanism of action by which these allosteric modulators promote disengagement of the motor from its microtubule track.

The hydrophobic domain created by an extended loop 5 and alpha helix 3 in the KSP motor domain accommodates a structurally diverse group of allosteric KSP inhibitors (Fig. 1) and is unique to class 5 kinesins.[1] Moreover, it has been proposed that the nonpolar nature of this pocket is unique to vertebrates.[1] Sequence alignments comparing the binding pockets of human, *Xenopus laevis*, and sea urchin *Strongylocentrotus purpuratus* revealed a high degree of sequence conservation between urchin and vertebrate KSP proteins, particularly at residues identified by mutational analysis to be critical for inhibition by monastrol and STLC analogs (Fig. 5A).[1–4] In contrast, the *Drosophila* homolog Klp61F was more

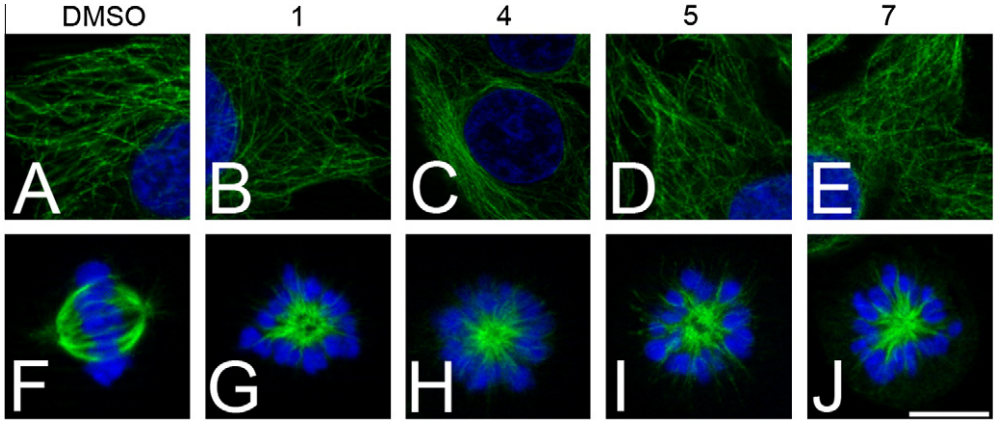

Figure 3. STLC analogs block bipolar spindle formation without affecting interphase microtubule organization. HeLa cells were incubated in the presence of 0.1% DMSO (A and F) or 1 μM STLC **1** (B and G), **4** (C and H), **5** (D and I), **7** (E and J) and then fixed and stained for microtubules (green) and DNA (blue).

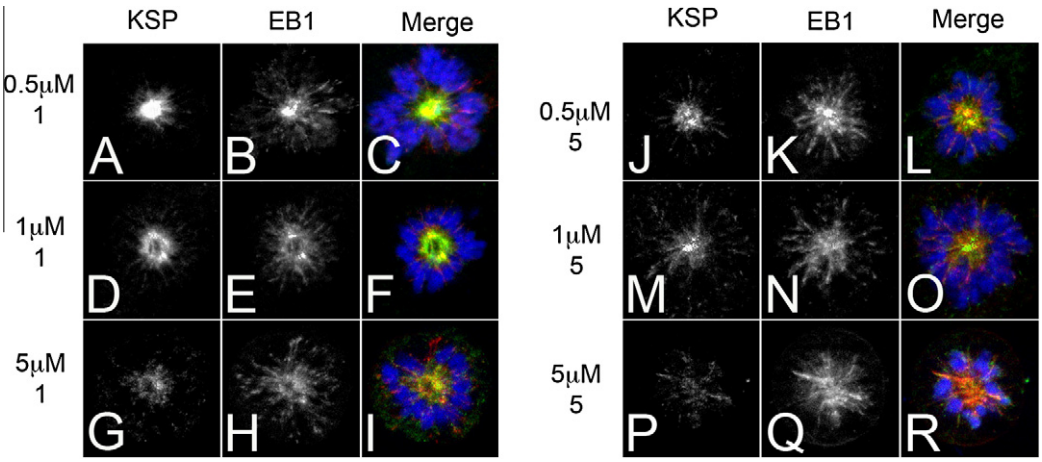

Figure 4. Dose-dependent depletion of KSP from monopolar spindles in 1 and 5-treated cells. HeLa cells were incubated in either **1** (A–I) or **5** (J–R) for 4 h and the fixed and processed for KSP (green), the microtubule-binding protein EB1 (red) and DNA (blue) localization, and images were acquired using equivalent exposure times for the green channel.

divergent, particularly within loop 5. To determine whether **1** or the cysteamine- or cysteinol derivatives were effective in sea urchin eggs or *Drosophila* S2 cells, cells were treated over a three log order range of concentrations, and scored for bipolar spindle formation by immunofluorescence. Compounds (**1–7**) were screened in S2 cells, however, no activity was detected at doses up to 100 μM and treatments extending up to 7 h (not shown).

In contrast, monopolar spindles were detected in *S. purpuratus* eggs treated during the first cell cycle following fertilization (Fig. 5B). Compound **5** blocked bipolar spindle formation with an EC_{50} of 28 μM, whereas the parent molecule **1** and monastrol were

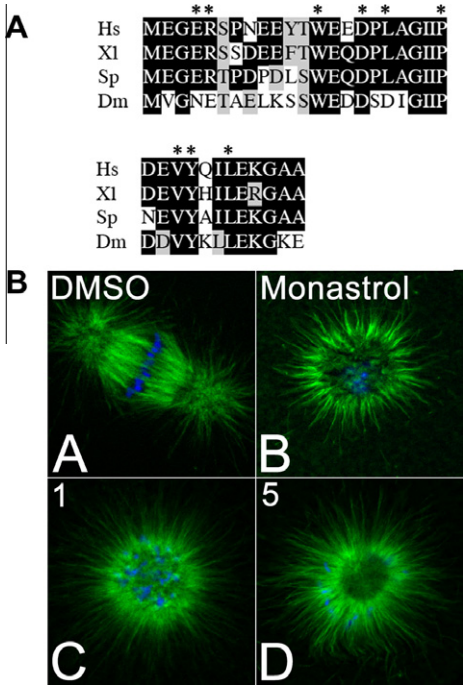

Figure 5. Efficacy of STLC derivatives in non-vertebrate organisms. (A) Alignment of the loop 5 (top) and helix 3 (bottom) of kinesin 5 homologs from *Homo sapiens* (NM_004523), *Xenopus laevis* (NM_001085956), *Strongylocentrotus purpuratus* (AF292395), and *Drosophila melanogaster* (NM_057470). Asterisks denote the residues reported to be required for drug inhibition.[1–4] (B) Micrographs of *S. purpuratus* eggs incubated in 100 μM Monastrol, **1**, or **5** and 0.1% DMSO as control. Eggs were fixed and processed for microtubule (green) and DNA (blue) localization.

weakly active with $EC_{50} \geqslant 100$ μM. The response to all compounds was phenotypically identical, causing spindle collapse following nuclear envelope breakdown resulting in a large monopolar spindle (Fig. 5B, panels B–D). Thus, the observed activity of these compounds in the highly ionic environment of seawater provides an additional assessment of the compounds biological efficacy using an invertebrate model organism, and the differences in activity between the compounds **1** and **5** in sea urchin eggs parallel the activities measured in human cultured cells.

Compounds **5** (MSTCO, NSC 747880) and **7** (MSTNH2, NSC 753791) were evaluated for anti-proliferative activity against the NCI60 tumor panel. Growth inhibitory concentrations (GI_{50}) of **5** and **7** ranged from 10 nM to 3 μM across the panel, with average GI_{50}'s of 360 and 350 nM for **5** and **7**, respectively (Table 2). This represented roughly a 143- and 35-fold average increase in potency over Monastrol (NSC 716782) and **1** (NSC 83265), respectively. There were, however, individual tumor lines such as melanoma M14 where **5** and **7** displayed a 1200-fold increase in activity over monastrol and the ovarian SK-OV-3 line where **5** and **7** displayed a 1250-fold increase in potency over the parent compound **1**. Thus, the tritylthioethanamine derivatives **5** and **7** had activities over a broad range of tumor types and represented a significant increase in anti-proliferative potency.

The possible binding modes of derivatives **5–7** were evaluated by molecular docking experiments using the crystal structure of human KSP (PBD: 2FME), and Genetic Optimization for Ligand Docking (Gold) scores were derived from 30 poses for each compound, with the highest scores illustrated in Figure 6. All three molecules docked into the binding pocket in the same manner, with the ammonium group forming hydrogen-bonding interactions with GLU 116 and GLY 117, consistent with previous docking studies for **1**.[39] Indeed, a structural of overlay of **1** with **7** revealed an identical alignment within the binding pocket (Fig. 6D). Similarly, the aromatic rings of the trityl groups for all three molecules fit into the previously described hydrophobic pockets (Hy1, comprised of TYR 211 and ALA 218 of α3; Hy2, comprised of ALA 133 of α2 at the base of loop 5; and Hy3, comprised of ILE 136 from α2, LEU 160, LEU 214 from α3). The highest scoring poses of **5**, **6** and **7** gave Gold scores of 85.74, 83.61, and 85.79, respectively. No specific interactions of the primary alcohol groups of **5** and **6** with the backbone of KSP were identified in these binding models.

Previously described studies as well as data reported here (Table 1) demonstrate an increase of potency for methoxytrityl derivatives of **1**.[39,40] While no specific interactions were identified for

Table 2
GI_{50} values [μM] from NCI60 panel screens* of Monastrol, **1**, **5**, and **7**

Cell line		Monastrol	**1**	**5**	**7**
Leukemia	CCRF-CEM	31.6	1.58	0.1	0.16
Leukemia	HL-60(TB)	25.1	2.51	0.19	0.25
Leukemia	K-562	31.6	1.58	0.06	0.04
Leukemia	MOLT-4	31.6	7.94	0.28	0.50
Leukemia	RPMI-8226	31.6	3.16	0.03	0.31
Leukemia	SR	31.6	6.31	0.01	0.13
NSC Lung	A549/ATCC	50.1	5.01	0.33	0.10
NSC Lung	EKVX	63.1	3.16	0.51	0.39
NSC Lung	HOP-62	63.1	19.9	0.51	0.66
NSC Lung	NCI-H226	50.1	100	2.75	1.74
NSC Lung	NCI-H23	63.1	2.51	0.26	0.51
NSC Lung	NCI-H322M	39.8	1.26	0.11	0.06
NSC Lung	NCI-H522	31.6	0.5	0.22	0.04
Colon	COLO 205	31.6	3.16	0.08	0.21
Colon	HCC-2998	39.8	2.51	0.05	0.24
Colon	HCT-116	31.6	0.5	0.03	0.04
Colon	HCT-15	39.8	2.51	0.21	0.05
Colon	HT29	79.4	3.98	0.34	0.35
Colon	KM12	31.6	5.01	0.22	0.31
Colon	SW-620	39.8	1.58	0.07	0.07
CNS	SF-268	63.1	3.98	0.11	0.15
CNS	SF-295	31.6	0.5	0.28	0.18
CNS	SF-539	50.1	0.79	0.26	0.25
CNS	SNB-19	79.4	2.51	0.25	0.34
CNS	SNB-75	39.8	1.99	0.26	0.60
CNS	U251	31.6	1	0.19	0.05
Melanoma	LOX IMVI	79.4	6.31	0.49	0.50
Melanoma	MALME-3M	63.1	1.26	0.36	0.22
Melanoma	M14	25.1	0.398	0.02	0.03
Melanoma	SK-MEL-2	31.6	1.5	0.24	0.06
Melanoma	SK-MEL-28	79.4	12.6	0.62	0.64
Melanoma	SK-MEL-5	39.8	0.63	0.06	0.05
Melanoma	UACC-257	63.1	1.26	0.54	0.70
Melanoma	UACC-62	39.8	1.99	0.25	0.40
Ovarian	IGROV1	50.1	3.98	0.26	0.15
Ovarian	OVCAR-3	50.1	2.51	0.2	0.15
Ovarian	OVCAR-4	63.1	12.6	1.62	1.40
Ovarian	OVCAR-5	79.4	100	0.39	0.57
Ovarian	OVCAR-8	63.1	1.99	0.42	0.12
Ovarian	SK-OV-3	63.1	100	0.08	0.08
Renal	786-0	63.1	1.26	0.44	0.40
Renal	ACHN	79.4	19.9	0.49	0.69
Renal	CAKI-1	63.1	15.8	0.45	0.19
Renal	SN12C	39.8	3.16	0.32	0.13
Renal	TK-10	100	6.31	0.46	1.56
Renal	UO-31	100	100	1.1	0.50
Average		51.5	12.6	0.36	0.35

* Cell lines shown are those common to all four screens.

the methoxy group and any side chains within the binding pocket, **5** and **7** demonstrated a slight preference for positioning the methoxyphenyl group in pocket Hy3 (Fig. 6A and C), while **6** preferred to occupy Hy1 (Fig. 6B), as illustrated by structural overlays of **5** and **6** (Fig. 6E). However, no poses showed the methoxyphenyl ring occupying pocket Hy2, the area nearest loop 5.

4. Discussion

The potential of kinesin inhibitors for use in the clinical arena is an area of active investigation, with several candidate drugs in clinical trials.[34,37,38,47] This study has identified *S*-trityl-derivatives of cysteinol and cysteamine as promising classes of selective KSP inhibitors. These compounds incorporate a small, flexible thioethanamine scaffold and exhibited increased activity as inhibitors of both purified recombinant motor activity as well as bipolar spindle assembly (Table 1). The increased potency of *para*-substitution of the trityl group in derivatives of **1** was maintained in the tritylthioethanamine compounds developed in this study. Previous modeling studies of **1** with KSP have indicated that these substituents are oriented towards the Hy3 hydrophobic pocket.[39] The tritylthioethanamine derivatives described here are able to establish additional interactions of the methoxy substituent with hydrophobic pockets 1 and 3, and preserve hydrogen bonding with the polar backbone contacts GLU116 and GLY117 that were identified as part of the pharmacophore.

The steric volume and hydrophobicity of the triphenylmethyl group are major determinants of the physicochemical and pharmacological properties of these compounds. It is intriguing to note the presence of the trityl moiety in a variety of compounds that have been identified as potential anti-cancer agents and function through different mechanisms of action.[48] 5′-*O*-Tritylinosine functions an allosteric inhibitor of the angiogenic enzyme thymidine phosphorylase.[49] The anti-fungal imidazole agent clotrimazole and synthetic analogs exhibit anti-cancer activity in cell culture and animal models, with treatment resulting in G1-phase arrest in the cell cycle, affecting intracellular Ca^{2++} levels and inducing detachment of mitochondrial-bound hexokinase that inhibits glycolysis.[50–53] Triphenylmethylamide derivatives have been shown to exhibit activity against multiple melanoma cell lines, causing G1-phase arrest and inducing apoptosis.[54,55] The related tritylphosphonate compound TPMP-III-2 exhibits anti-cancer activity and induces arrest in the M-phase of the cell cycle with characteristic formation of fragmented mitotic spindles, through inhibition of tubulin polymerization.[48] In contrast, inhibition of KSP by STLC derivatives results in M phase cell cycle arrest and is characterized by the formation of the monopolar spindle. Synthetic diphenylheterocyclic carbinols derivatives were recently shown to exhibit anti-proliferative effects against carcinoma cell lines.[56] The cysteamine and cysteinol derivatives described herein are shown to be effective inhibitors of KSP and exhibit the archetypal monopolar phenotype, demonstrating the importance of both the trityl- and ethanamine elements of the pharmacophore.

Methoxytritylethanamine derivatives demonstrated improved efficacy in blocking KSP ATPase activity and bipolar spindle assembly in HeLa cells (Table 1). The zwitterionic character and neutral overall charge of carboxylic derivatives **1**–**3** represents major physicochemical differences, with respect to compounds **4**–**7**, that possess positive charges due to their protonated amine groups at physiological pH. In order to evaluate our lead compounds against an expanded panel of tumor cell types, **5** and **7** were submitted to the NCI Developmental Therapeutics Program to be screened against the NCI60 tumor panel.

Examination of the growth inhibitory activities in cell lines common to screens of monastrol, **1**, **5**, and **7** revealed that the ethanamine derivatives showed greater efficiency in blocking tumor cell growth in comparison to **1** and monastrol (Table 2). Leukemia and colon tumor cell lines were generally the most susceptible, with average GI_{50} values $\leqslant$230 nM for both compounds. Indeed, the differential sensitivity of hematological neoplasms to KSP inhibitors has been noted for other compounds, and several of these compounds have advanced through preclinical evaluation.[47,57–61] Thus, the cysteinol and cysteamine scaffolds hold promise for further development as therapeutically useful anti-proliferative agents.

As an additional means of studying the interaction between these compounds and the KSP motor domain, analogs were tested against diverse species that contain varying degrees of conservation within the inhibitor-binding pocket (Fig. 5). A single report has described monastrol- and **1** efficacy in a brown algae,[62] but there have been no other examples of KSP inhibitors functioning in invertebrate cells. Examination of the loop 5 and helix 3 reveal that while sea urchin KSP shares a high degree of identity with human KSP throughout the binding pocket, including the residues identified as being essential for inhibition by **1**, as well as monastrol and ispinesib (Fig. 5A, asterisks). In contrast, the *Drosophila*

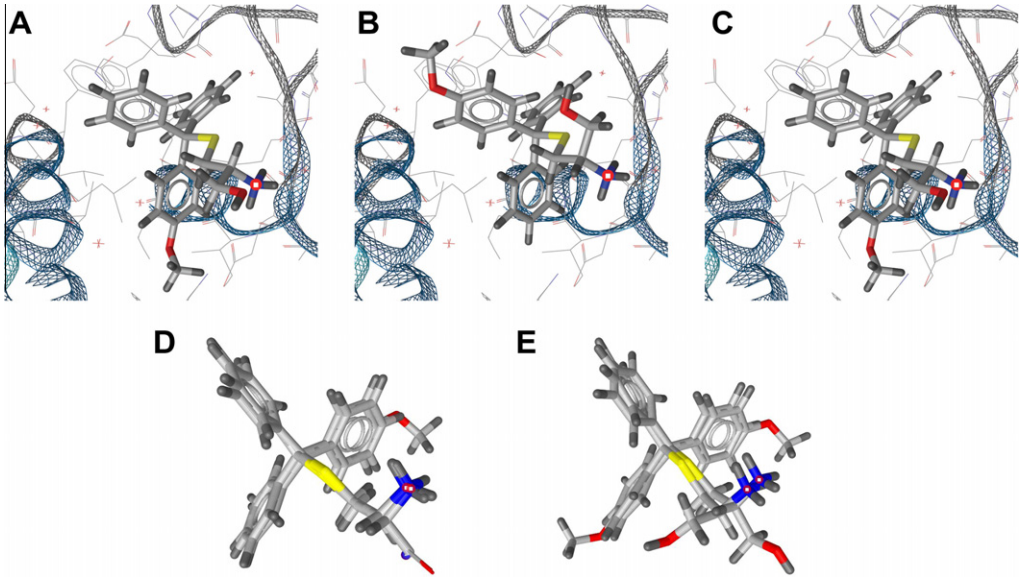

Figure 6. Docking studies of compounds **5**–**7**. Highest scoring poses of **5** (A), **6** (B), and **7** (C) in the allosteric binding site of KSP (PDB: 2FME). All inhibitors bind to the same pocket formed by loop 5, α2 and α3. Helix α3 is shown to the left and loop 5 defines the right side and upper lid of the site. (D) Overlay of optimal poses for **1** and **7**; (E) overlay of the *R*- and *S*-enantiomers **5** and **6**.

homolog Klp61F shares only partial identity with echinoderm and vertebrate loop 5, with notable variation at positions 116, 117, and 130, residues identified as crucial for monastrol- and STLC inhibition in human KSP.[1–4] Indeed, whereas we found that derivatives of STLC were effective in sea urchin eggs (Fig. 5B), *Drosophila* S2 cells were resistant to all compounds tested (not shown). However, because Klp61F contains a serine residue position 129 that is a proline in vertebrate KSP homologs, it is possible that this variation alters the structure of loop 5 and thus Hy2. Thus, understanding the structural differences between vertebrate and invertebrate KSP homologs may lead to opportunities for the rational design of inhibitors that selectively target nonmammalian pathogens.

5. Conclusions

Derivatization of both the cysteine and triphenylmethyl groups of known KSP inhibitor **1** has provided a new class of compounds that display increased potency in both biochemical and cell-based assays. The structure-based mechanism of action exhibited by this class of triphenylmethyl derivatives with respect to **1** is maintained by these compounds, eliciting cell cycle arrest and producing the characteristic monoaster spindle phenotype that results from KSP inhibition. The cysteinol and cysteamine derivatives **5** and **7** displayed an average thirty five-fold increase anti-proliferative activity against the NCI60 panel of cancer cell lines in comparison with **1**, as well as broadened species specificity. The potent activity and conformational flexibility of these small molecule allosteric inhibitors of KSP offers real promise for applications as research tools and potential for further development as clinically useful anti-tumor agents.

6. Experimental

6.1. General methods

All reactions were performed in an efficient fume hood. Commercially available solvents and reagents were used without further purification. Preparative chromatographic separations were performed using medium pressure flash chromatography and ethyl acetate/hexanes or methanol/dichloromethane as eluent. Reverse phase chromatography employed C-18 columns and water–acetonitrile or water–methanol mobile phase. NMR spectra were acquired at ambient temperatures (18 ± 2 °C) unless otherwise noted. Reactions were monitored by thin-layer chromatography on silica gel (60 Å pore size, 5–17 μm) polyester backed sheets that were visualized under a UV lamp, iodine vapor, phosphomolybdic acid, or anisaldehyde. The ^{1}H NMR spectra in $CDCl_3$ were referenced to TMS unless otherwise noted. The ^{13}C $\{^{1}H\}$ NMR spectra were recorded at 75 or 100 MHz and referenced relative to the ^{13}C $\{^{1}H\}$ peaks of the solvent. NMR spectra are reported as ppm (δ), (multiplicity, coupling constants (Hz), and number of protons). Infrared spectra were recorded as KBr pellets or neat films and are reported in cm^{-1}. Melting points are uncorrected. The purity of all compounds used in biological studies was determined to be >95% by analytical HPLC equipped with Photodiode Array (PDA) and ESI-MS detection. The compounds (1 mg/mL CH_3CN, 20 μL) were injected into a Waters Symmetry® C_{18} 5 μm 3.0 × 150 mm column and eluted as specified. Compound STLC (**1**) was obtained from Novabiochem, Compounds **2**,[40] **3**,[40] and **7**[43] were prepared following reported procedures. The other compounds were synthesized as follows.

6.1.1. General procedure for the preparation of *S*-triarylmethyl-cysteinol (4–6)

Borane-THF (4 mL, 4 mmol) was added dropwise to cysteine (0.121 g, 1 mmol) in dryTHF (5 mL) at 0 °C under an argon atmosphere, and stirred at room temperature for 7 h. The reaction mixture was quenched with dry DMF (1 mL) and stirred for 1 h. Triarylmethylchloride (0.5 mmol) was added to the reaction mixture and stirred at room temperature for 3 h. The volatiles were removed in vacuo. The residue was dissolved in CH_2Cl_2 (20 mL), washed with H_2O (20 mL), saturated NaCl solution (10 mL), and dried over Na_2SO_4. The solvents were evaporated under reduced pressure and the residue was purified by silica gel chromatography using CH_3OH/CH_2Cl_2 (3:97) as eluent to isolate the product.

6.1.2. (*R*)-2-amino-3-(tritylthio)propan-1-ol (4)

From L-cysteine and trityl chloride; yield (88%) as colorless viscous oil. IR (KBr, cm^{-1}): 3425, 3054, 2917, 1593, 742; ^{1}H NMR

(300 MHz, $CDCl_3$) δ 7.44–7.39 (m, 6H), 7.31–7.17 (m, 9H), 3.38 (dd, J = 10.86, 4.26 Hz, 1H), 3.15 (dd, J = 10.71, 6.89 Hz, 1H), 2.61–2.53 (m, 1H), 2.31 (dd, J = 12.47, 5.14 Hz, 1H), 2.20 (dd, J = 12.47, 7.63 Hz, 1H), 1.52 (s, 3H); ^{13}C NMR (75 MHz, $CDCl_3$) δ 144.60, 129.50, 127.84, 126.67, 66.77, 65.53, 51.99, 36.62. HPLC–MS: Elution with CH_3CN/H_2O (20:80) exhibited a single peak at 3.92 min. ESI-MS m/z [ES^+] calcd for $C_{22}H_{24}NOS$ $[M+H]^+$ 350.44; found 350.16.

6.1.3. (*R*)-2-amino-3-((4-methoxyphenyl)diphenylmethylthio) propan-1-ol (5)

From L-cysteine and 4-methoxytrityl chloride; yield (91%) as colorless viscous oil. $[\alpha]_D^{20}$ +6.91° (c 0.57, $CHCl_3$); IR (Neat, cm^{-1}): 3447, 2925, 1508, 1250, 1033; ^1H NMR (300 MHz, $CDCl_3$) δ 7.42–7.17 (m, 12H), 6.81 (d, J = 8.8 Hz, 2H), 3.79 (s, 3H), 3.44–3.39 (dd, J = 10.71, 4.11 Hz, 1H), 3.21–3.15 (m, 1H), 2.65–2.55 (m, 1H), 2.36–2.19 (m, 2H), 1.55 (s, 3H); ^{13}C NMR (75 MHz, $CDCl_3$) δ 158.10, 144.95, 136.76, 130.72, 129.46, 127.87, 126.64, 113.14, 66.36, 65.72, 55.11, 52.06, 36.85. HPLC–MS: Elution with CH_3CN/H_2O (20:80), exhibited a single peak at 2.18 min. ESI-MS m/z [ES^+] calcd for $C_{29}H_{26}NO_2S$ $[M+H]^+$ 380.09; found 380.16. HRMS calcd 380.1679; found 380.1678.

6.1.4. (*S*)-2-amino-3-((4-methoxyphenyl)diphenylmethylthio) propan-1-ol (6)

From D-cysteine and 4-methoxytrityl chloride; yield (92%) as colorless viscous oil. $[\alpha]_D^{20}$ −6.04° (c 0.57, $CHCl_3$); IR (Neat, cm^{-1}): 3447, 2925, 1508, 1250, 1033; ^1H NMR (300 MHz, $CDCl_3$) δ 7.42–7.17 (m, 12H), 6.81 (d, J = 8.8 Hz, 2H), 3.79 (s, 3H), 3.44–3.39 (dd, J = 10.71, 4.11 Hz, 1H), 3.21–3.15 (m, 1H), 2.65–2.55 (m, 1H), 2.36–2.19 (m, 2H), 1.54 (s, 3H); ^{13}C NMR (75 MHz, $CDCl_3$) δ 158.10, 144.89, 136.70, 130.72, 129.46, 127.87, 126.67, 113.14, 66.36, 65.72, 55.20, 52.06, 36.81. HPLC–MS: Elution with 20–80% CH_3CN in H_2O (gradient 1.5% min^{-1}), exhibited a single peak at 2.18 min. ESI-MS m/z [ES^+] calcd for $C_{29}H_{26}NO_2S$ $[M+H]^+$ 380.09; found 380.16.

6.2. Analysis of analogs using an in vitro kinesin end-point ATPase assay

Inhibitory activity of STLC analogs were measured using a microtubule-activated ATPase end-point assay from Cytoskeleton (Denver, CO). The reagents and kinesin motor domains were added to wells of a 96-well microtitre dish (Greiner Bio-One, Monroe, NC) in a total reaction volume of 30 μL. Reactions were started by the addition of 2 mM ATP (Sigma Co., St Louis, MO), incubated at room temperature for 5 min, and terminated by the addition of 70 μL of CytoPhos. The reactions were incubated for an additional 10 min at room temperature and absorbance was measured at 650 nm using a microplate reader Elx 800™ (BIO-TEK® Winooski, VT) at 650 nm. All kinesin domain motors were used at a final concentration of 0.08 μg/μL. STLC and its derivatives were assayed over a range of concentrations between 0.25 μM to 10 μM. Controls of DMSO were used at a final concentration of 0.1%. All conditions were performed in triplicate, and raw data was entered into Graphpad Prism software, and IC_{50} values were calculated using a four parameter nonlinear regression.

6.3. Mammalian cell culture

HeLa cells (American Type Culture Collection, Manassas, VA) were cultured in minimum essential medium with Earle's BSS (Lonza, Walkersville, MD), supplemented with 10% fetal bovine serum, 1% penicillin/streptomycin, fungicide, 1.5 g/L sodium bicarbonate, and 1.0 mM sodium pyruvate (Sigma Chemical Co., St. Louis, MO) in 5% CO_2 at 37 °C in a humidified incubator. STLC and its derivatives were screened for KSP inhibition by incubating cells for four hours with either carrier alone (0.1% DMSO) or DMSO-solublized compound in doses ranging from 50 nM to 100 μM. Cells were then processed for tubulin and DNA localization and 100 mitotic cells were scored for bipolar spindle formation per condition. EC_{50} values were calculated using Graphpad Prism software using a four parameter nonlinear regression as described above. Growth inhibitory activity of tumor cell lines (NCI60 panel) was performed by the Developmental Therapeutics Program, Division of Cancer Treatment and Diagnosis, National Cancer Institute, U.S.A.

6.4. Sea urchin embryo culture

S. purpuratus sea urchins were obtained from Marinus (Long Beach, CA) and maintained in chilled aquarium at 10 °C. Gametes were obtained by intracoloemic injection of 0.5 M KCl and eggs were fertilized in artificial seawater in the presence of 2 mM 3-amino triazole to prevent hardening of the fertilization envelope. Twenty minutes after fertilization, eggs were stripped of their fertilization envelops by passage through 80 μm Nitex, and cultured either in the presence of 0.1% DMSO or KSP inhibitors. At the time of first mitosis, eggs were fixed and processed for microtubule and DNA localization as previously described.[63] To generate EC_{50} values for KSP inhibitor activity in sea urchin eggs, embryos were treated over a three log order range of concentrations from 100 nM to 100 μM, processed for microtubule localization, and then scored for bipolar spindle formation (100 cells scored per condition).

6.5. Immunofluorescence

Hela cells were incubated in the presence of compounds dissolved in DMSO at the specified concentration for 4 h and then fixed by immersion in 100% MeOH for a minimum of thirty minutes at −20 °C before rehydration in phosphate-buffered saline (PBS) for 10 min. Hela cells were blocked by incubation in PBS containing 5% Bovine Serum Albumin (PBS-BSA) for 1 hour at room temperature. Cells were then probed with either mouse anti-tubulin (Sigma, Co, St. Louis, MO), or mouse anti-KSP (Abcam, Cambridge, MA) in blocking buffer overnight at 4 °C. To counterstain the microtubule cytoskeleton in KSP localization experiments, cells were also probed for the presence of the microtubule end-binding protein EB1 using a custom rabbit polyclonal antibody against whole recombinant human EB1 (Pro-Sci, Poway, CA). Primary antibodies were detected using AlexaFluor-conjugated secondary antibodies (Molecular Probes, Eugene OR). After washing, cells were mounted in 90% glycerol/1× PBS and imaged using a Zeiss 200 M inverted microscope equipped with epifluorescence optics and an Apotome structured illumination module, a 100 W mercury arc fluorescent light source and DAPI, FITC, and TRITC filter sets. Images were acquired using a 63× 1.4 NA Plan-aprochromat objective, an Axiocam MrM 12 bit CCD camera driven by Axiovision 4.5 software. Images were exported as 8 bit tif images and figures were prepared using Adobe Photoshop® software.

6.6. In silico docking studies

All docking calculations were performed on a PC equipped with a 1.6 GHz Core 2 duo processor and 4 GB of RAM, running Windows 7. Ligand structures were generated using Spartan' 10.0 (Wavefunction Inc., Irvine, CA), including expected protonation states at physiological pH, and geometry optimized. Binding site preparation of the KSP complexes and docking studies were performed with Gold Suite 5.0.1 (The Cambridge Crystallographic Data

Centre: Cambridge U.K., 2010) and Hermes 1.4.1. Docking was performed in the binding site of PDB code: 2FME. All the water molecules present in the binding site were allowed to be replaced by the ligand or to change orientation. The standard function Gold score was used for ranking the poses, including 30 solutions for each ligand generated. Ligand Scout v 3.0 (Inte:Ligand GmbH: Vienna, Austria, 2010) was used for visual inspection of the docked poses and for producing three-dimensional visual representations.

Acknowledgments

The authors would like to thank Dr. Kathy Hanley for her assistance in statistical analyses. This work is supported by National Science Foundation MCB0818729 (CBS), National Center for Research Resources P20 RR16480 (JBA and CBS), the Howard Hughes Medical Institute's Undergraduate Education Improvement Program at NMSU, the Cowboys for Cancer Research Foundation, and an Interdisciplinary Research Grant from the NMSU Vice President for Research (JBA and CBS). We acknowledge the NCI Developmental Therapeutics Program for providing biological data including NCI60 screening services, see http://dtp.cancer.gov/.

Supplementary data

Supplementary data associated with this article can be found, in the online version, at doi:10.1016/j.bmc.2011.07.054.

References and notes

1. Maliga, Z.; Mitchison, T. J. *BMC Chem. Biol.* **2006**, *6*, 2.
2. Marshall, C. G.; Torrent, M.; Williams, O.; Hamilton, K. A.; Buser, C. A. *Arch. Biochem. Biophys.* **2009**, *484*, 1.
3. Tcherniuk, S.; van Lis, R.; Kozielski, F.; Skoufias, D. A. *Biochem. Pharmacol* **2009**, *79*, 864.
4. Brier, S.; Lemaire, D.; DeBonis, S.; Forest, E.; Kozielski, F. *J. Mol. Biol.* **2006**, *360*, 360.
5. Jordan, M. A.; Wilson, L. *Nat. Rev. Cancer* **2004**, *4*, 253.
6. Zhou, J.; Giannakakou, P. *Curr. Med. Chem. Anticancer Agents* **2005**, *5*, 65.
7. Bergnes, G.; Brejc, K.; Belmont, L. *Curr. Top. Med. Chem.* **2005**, *5*, 127.
8. Duhl, D. M.; Renhowe, P. A. *Curr. Opin. Drug Discov. Devel.* **2005**, *8*, 431.
9. Huszar, D.; Theoclitou, M. E.; Skolnik, J.; Herbst, R. *Cancer Metastasis Rev.* **2009**, *28*, 197.
10. Knight, S. D.; Parrish, C. A. *Curr. Top. Med. Chem.* **2008**, *8*, 888.
11. Zhang, Y.; Xu, W. *Anticancer Agents Med. Chem.* **2008**, *8*, 698.
12. Lawrence, C. J.; Dawe, R. K.; Christie, K. R.; Cleveland, D. W.; Dawson, S. C.; Endow, S. A.; Goldstein, L. S.; Goodson, H. V.; Hirokawa, N.; Howard, J.; Malmberg, R. L.; McIntosh, J. R.; Miki, H.; Mitchison, T. J.; Okada, Y.; Reddy, A. S.; Saxton, W. M.; Schliwa, M.; Scholey, J. M.; Vale, R. D.; Walczak, C. E.; Wordeman, L. *J. Cell Biol.* **2004**, *167*, 19.
13. Goshima, G.; Vale, R. D. *J. Cell Biol.* **2003**, *162*, 1003.
14. Blangy, A.; Lane, H. A.; d'Herin, P.; Harper, M.; Kress, M.; Nigg, E. A. *Cell* **1995**, *83*, 1159.
15. Mountain, V.; Simerly, C.; Howard, L.; Ando, A.; Schatten, G.; Compton, D. A. *J. Cell Biol.* **1999**, *147*, 351.
16. Skoufias, D. A.; DeBonis, S.; Saoudi, Y.; Lebeau, L.; Crevel, I.; Cross, R.; Wade, R. H.; Hackney, D.; Kozielski, F. *J. Biol Chem.* **2006**, *281*, 17559.
17. Haque, S. A.; Hasaka, T. P.; Brooks, A. D.; Lobanov, P. V.; Baas, P. W. *Cell Motil. Cytoskeleton* **2004**, *58*, 10.
18. Mayer, T. U.; Kapoor, T. M.; Haggarty, S. J.; King, R. W.; Schreiber, S. L.; Mitchison, T. J. *Science* **1999**, *286*, 971.
19. DeBonis, S.; Skoufias, D. A.; Lebeau, L.; Lopez, R.; Robin, G.; Margolis, R. L.; Wade, R. H.; Kozielski, F. *Mol. Cancer Ther.* **2004**, *3*, 1079.
20. Zee-Cheng, K. Y.; Cheng, C. C. *J. Med. Chem.* **1970**, *13*, 414.
21. Tarby, C. M.; Kaltenbach, R. F., 3rd; Huynh, T.; Pudzianowski, A.; Shen, H.; Ortega-Nanos, M.; Sheriff, S.; Newitt, J. A.; McDonnell, P. A.; Burford, N.; Fairchild, C. R.; Vaccaro, W.; Chen, Z.; Borzilleri, R. M.; Naglich, J.; Lombardo, L. J.; Gottardis, M.; Trainor, G. L.; Roussell, D. L. *Bioorg. Med. Chem. Lett.* **2006**, *16*, 2095.
22. Cox, C. D.; Coleman, P. J.; Breslin, M. J.; Whitman, D. B.; Garbaccio, R. M.; Fraley, M. E.; Buser, C. A.; Walsh, E. S.; Hamilton, K.; Schaber, M. D.; Lobell, R. B.; Tao, W.; Davide, J. P.; Diehl, R. E.; Abrams, M. T.; South, V. J.; Huber, H. E.; Torrent, M.; Prueksaritanont, T.; Li, C.; Slaughter, D. E.; Mahan, E.; Fernandez-Metzler, C.; Yan, Y.; Kuo, L. C.; Kohl, N. E.; Hartman, G. D. *J. Med. Chem.* **2008**, *51*, 4239.
23. Lad, L.; Luo, L.; Carson, J. D.; Wood, K. W.; Hartman, J. J.; Copeland, R. A.; Sakowicz, R. *Biochemistry* **2008**, *47*, 3576.
24. Nakai, R.; Iida, S.; Takahashi, T.; Tsujita, T.; Okamoto, S.; Takada, C.; Akasaka, K.; Ichikawa, S.; Ishida, H.; Kusaka, H.; Akinaga, S.; Murakata, C.; Honda, S.; Nitta, M.; Saya, H.; Yamashita, Y. *Cancer Res.* **2009**, *69*, 3901.
25. Brier, S.; Lemaire, D.; Debonis, S.; Forest, E.; Kozielski, F. *Biochemistry* **2004**, *43*, 13072.
26. Brier, S.; Lemaire, D.; DeBonis, S.; Kozielski, F.; Forest, E. *Rapid Commun. Mass Spectrom.* **2006**, *20*, 456.
27. Maliga, Z.; Kapoor, T. M.; Mitchison, T. J. *Chem. Biol.* **2002**, *9*, 989.
28. Maliga, Z.; Xing, J.; Cheung, H.; Juszczak, L. J.; Friedman, J. M.; Rosenfeld, S. S. *J. Biol. Chem.* **2006**, *281*, 7977.
29. Turner, J.; Anderson, R.; Guo, J.; Beraud, C.; Fletterick, R.; Sakowicz, R. *J. Biol. Chem.* **2001**, *276*, 25496.
30. Cochran, J. C.; Gilbert, S. P. *Biochemistry* **2005**, *44*, 16633.
31. Behnke-Parks, W. M.; Vendome, J.; Honig, B.; Maliga, Z.; Moores, C.; Rosenfeld, S. S. *J. Biol. Chem.* **2011**, *286*, 5242.
32. Kim, E. D.; Buckley, R.; Learman, S.; Richard, J.; Parke, C.; Worthylake, D. K.; Wojcik, E. J.; Walker, R. A.; Kim, S. *J. Biol. Chem.* **2010**, *285*, 18650.
33. Beer, T. M.; Goldman, B.; Synold, T. W.; Ryan, C. W.; Vasist, L. S.; Van Veldhuizen, P. J., Jr.; Dakhil, S. R.; Lara, P. N., Jr.; Drelichman, A.; Hussain, M. H.; Crawford, E. D. *Clin. Genitourin. Cancer* **2008**, *6*, 103.
34. Lee, C. W.; Belanger, K.; Rao, S. C.; Petrella, T. M.; Tozer, R. G.; Wood, L.; Savage, K. J.; Eisenhauer, E. A.; Synold, T. W.; Wainman, N.; Seymour, L. *Invest. New Drugs* **2008**, *26*, 249.
35. Blagden, S. P.; Molife, L. R.; Seebaran, A.; Payne, M.; Reid, A. H.; Protheroe, A. S.; Vasist, L. S.; Williams, D. D.; Bowen, C.; Kathman, S. J.; Hodge, J. P.; Dar, M. M.; de Bono, J. S.; Middleton, M. R. *Br. J. Cancer* **2008**, *98*, 894.
36. Kathman, S. J.; Williams, D. H.; Hodge, J. P.; Dar, M. *Cancer Chemother. Pharmacol.* **2009**, *63*, 469.
37. Knox, J. J.; Gill, S.; Synold, T. W.; Biagi, J. J.; Major, P.; Feld, R.; Cripps, C.; Wainman, N.; Eisenhauer, E.; Seymour, L. *Invest. New Drugs* **2008**, *26*, 265.
38. Tang, P. A.; Siu, L. L.; Chen, E. X.; Hotte, S. J.; Chia, S.; Schwarz, J. K.; Pond, G. R.; Johnson, C.; Colevas, A. D.; Synold, T. W.; Vasist, L. S.; Winquist, E. *Invest. New Drugs* **2008**, *26*, 257.
39. Debonis, S.; Skoufias, D. A.; Indorato, R. L.; Liger, F.; Marquet, B.; Laggner, C.; Joseph, B.; Kozielski, F. *J. Med. Chem.* **2008**, *51*, 1115.
40. Ogo, N.; Oishi, S.; Matsuno, K.; Sawada, J.; Fujii, N.; Asai, A. *Bioorg. Med. Chem. Lett.* **2007**, *17*, 3921.
41. Kaan, H. Y.; Weiss, J.; Menger, D.; Ulaganathan, V.; Tkocz, K.; Laggner, C.; Popowycz, F.; Joseph, B.; Kozielski, F. *J. Med. Chem.* **2011**, *54*, 1576.
42. Hapuarachchige, S.; Montano, G.; Ramesh, C.; Rodriguez, D.; Henson, L. H.; Williams, C. C.; Kadavakkollu, S.; Johnson, D. L.; Shuster, C. B.; Arterburn, J. B. *J. Am. Chem. Soc.* **2011**, *133*, 6780.
43. Riddoch, R. W.; Schaffer, P.; Valliant, J. F. *Bioconjugate Chem.* **2006**, *17*, 226.
44. Funk, C. J.; Davis, A. S.; Hopkins, J. A.; Middleton, K. M. *Anal. Biochem.* **2004**, *329*, 68.
45. Cochran, J. C.; Gatial, J. E., 3rd; Kapoor, T. M.; Gilbert, S. P. *J. Biol. Chem.* **2005**, *280*, 12658.
46. Kapoor, T. M.; Mayer, T. U.; Coughlin, M. L.; Mitchison, T. J. *J. Cell Biol.* **2000**, *150*, 975.
47. Carol, H.; Lock, R.; Houghton, P. J.; Morton, C. L.; Kolb, E. A.; Gorlick, R.; Reynolds, C. P.; Maris, J. M.; Keir, S. T.; Billups, C. A.; Smith, M. A. *Pediatr. Blood Cancer* **2009**, *53*, 1255.
48. Palchaudhuri, R.; Nesterenko, V.; Hergenrother, P. J. *J. Am. Chem. Soc.* **2008**, *130*, 10274.
49. Casanova, E.; Hernandez, A. I.; Priego, E. M.; Liekens, S.; Camarasa, M. J.; Balzarini, J.; Perez-Perez, M. J. *J. Med. Chem.* **2006**, *49*, 5562.
50. Al-Qawasmeh, R. A.; Lee, Y.; Cao, M. Y.; Gu, X.; Vassilakos, A.; Wright, J. A.; Young, A. *Bioorg. Med. Chem. Lett.* **2004**, *14*, 347.
51. Benzaquen, L. R.; Brugnara, C.; Byers, H. R.; Gatton-Celli, S.; Halperin, J. A. *Nat. Med.* **1995**, *1*, 534.
52. Khalid, M. H.; Tokunaga, Y.; Caputy, A. J.; Walters, E. *J. Neurosurg.* **2005**, *103*, 79.
53. Snajdrova, L.; Xu, A.; Narayanan, N. *J. Biol. Chem.* **1998**, *273*, 28032.
54. Dothager, R. S.; Putt, K. S.; Allen, B. J.; Leslie, B. J.; Nesterenko, V.; Hergenrother, P. J. *J. Am. Chem. Soc.* **2005**, *127*, 8686.
55. Palchaudhuri, R.; Hergenrother, P. J. *Bioorg. Med. Chem. Lett.* **2008**, *18*, 5888.
56. Benaka Prasad, S.; Vinaya, K.; Ananda Kumar, C.; Swarup, S.; Rangappa, K. *Med. Chem. Res.* **2010**, *19*, 220.
57. Shi, J.; Orth, J. D.; Mitchison, T. *Cancer Res.* **2008**, *68*, 3269.
58. Kantarjian, H. M.; Padmanabhan, S.; Stock, W.; Tallman, M. S.; Curt, G. A.; Li, J.; Osmukhina, A.; Wu, K.; Huszar, D.; Borthukar, G.; Faderl, S.; Garcia-Manero, G.; Kadia, T.; Sankhala, K.; Odenike, O.; Altman, J. K.; Minden, M. *Invest New Drugs* **2011**. doi:10/1007/s10637-011-9660-2.
59. Shimizu, M.; Ishii, H.; Ogo, N.; Unno, Y.; Matsuno, K.; Sawada, J.; Akiyama, Y.; Asai, A. *Cancer Lett.* **2010**, *298*, 99.
60. Tunquist, B. J.; Woessner, R. D.; Walker, D. H. *Mol. Cancer Ther.* **2010**, *9*, 2046.
61. Carter, B. Z.; Mak, D. H.; Woessner, R.; Gross, S.; Schober, W. D.; Estrov, Z.; Kantarjian, H.; Andreeff, M. *Leukemia* **2009**, *23*, 1755.
62. Peters, N. T.; Kropf, D. L. *BMC Plant Biol.* **2006**, *6*, 19.
63. George, O.; Bryant, B. K.; Chinnasamy, R.; Corona, C.; Arterburn, J. B.; Shuster, C. B. *ACS Chem. Biol.* **2008**, *3*, 167.